EPJ Web of Conferences **29**, 00048 (2012)
DOI: 10.1051/epjconf/20122900048

Structural characterization of mechanically alloyed nanocrystalline Cu-Fe: Strain broadening due to dislocations

M. Azabou[1], L. Escoda[2], J. J. Sunol[2] and M. Khitouni[1,a],

[1]Laboratoire de Chimie Inorganique, 99/UR/12-22, Université de Sfax, BP 1171, 3018-Sfax, Tunisia
[2]Dep. de Fisica, Universitat de Girona, Campus Montilivi, Girona 17071, Spain

Abstract. Nanocrystalline Cu(Fe) solid solution was successfully synthesized by using high-energy mechanical milling. The structural and morphological changes during mechanical milling were investigated by X-ray diffraction and scanning electron microscopy. The patterns so obtained were analyzed using the X'Pert High Score Plus program. The final product of the mechanical alloying process was nanocrystalline FCC Cu(Fe) solid solution with a mean crystallite size in the range of few nanometers. The final microstructure, especially the high levels of lattice strains was explained by the presence of dislocations, with a dislocation density of about 7.4×10^{16} m^{-2}. The identified steady-state saturation values of these parameters can be related to accumulate strain hardening of the powder material during longer milling times.

1 Introduction

Mechanical alloying (MA) is a solid state process in which the powder mixtures are mechanically milled by balls with high energy. This method was usually used to synthesized supersaturated solid solution (SSS), quasi-crystalline (QC), nanocrystalline and amorphous alloys [1–4]. Their advantages (relatively low-temperature processing, easy control of compositions, relatively inexpensive equipments needed...) greatly facilitate the characterization and application of the resulting metastable alloys. The Fe-Cu system is an example of a binary system with a low solid miscibility at room temperature (a miscibility of approximately 3%). Shingu et al. [5] Uenishi et al. [6] and Yavari et al. [1] were the first to report the formation of metastable solid solutions in the Fe-Cu system by MA. Eckert et al. [7] have reported that single phase FCC alloys and single phase BCC alloys are formed by MA in the FexCu100-x system with x<60 and with x>80, respectively. Moreover, Majumdar et al. [8] and Gaffet et al. [9] have deduced that the formation of the BCC Fe-Cu solid solution is restricted to 0-20 wt% Cu. According to their investigation, this process occurred in two steps: a nanocrystallization step and an Fe(Cu) and/or Cu(Fe) formation step. In all studied powders, these authors found that the grain size of prepared solid solutions was in the nanometer range and the lattice strain increased with milling time. These variations of structural parameters may be understood in terms of the various deformation mechanisms occurring and the way these create defects within the solid solution. Subsequently, a few amount of work has been done on the

[a] e-mail : khitouni@yahoo.fr

mechanism of formation of metastable Fe-Cu solid solutions by MA. However, only a few reports are available in literature [10, 11] on the structure defects in nanostructured Fe-Cu alloys. Although kinetics are faster in nanoscale, our recent experiments [12] based on the Angar et al. approach [13,14] demonstrate that strain broadening caused by high energy MA is consistent with the concept of dislocations. So, the variations of structural parameters may be understood in terms of the various deformation and annealing mechanisms occurring and the way these create or eliminate defects within the solid solution [15, 16].

The aim of this paper was to study the structural transformations taking place during MA of the Cu-40 at% Fe powder mixture in a high energy ball mill. The obtained results provide additional insight into the mechanism formation of the solid solution in the Cu-Fe system and demonstrate that strain broadening caused by high energy mechanical alloying is due to dislocations.

2 Experimental

Pure elemental powders, Cu (99.9%) and Fe (99.3%), with, respectively, 85 and 75 μm particle sizes, were separately weighed and mixed to get the desired composition (Cu-40at% Fe). Mechanical alloying was carried out in a planetary ball mill (Retsch PM 400) at room temperature, using flasks made of hardened steel balls. The milling was performed, in argon atmosphere, at speed of Ω =400 rpm. Samples were collected from the vials after regular time intervals during milling for further investigations. The phase identification of the milled samples was examined by X-ray diffraction (XRD) using CuKα1 radiation in a Siemens D5000 X-ray diffractometer. The X-ray diffraction data was collected at a slow scan rate of 0.016°/4s for the careful determination of microstructural parameters of the milled powders. The morphology and composition study were done via scanning electron microscopy in a DSM960A ZEISS microscope with energy dispersive X-ray microanalysis (EDX).

3 Results and discussions

3.1 Morphology and particle size analysis

Figure 1 shows typical scanning electron microscopy (SEM) images of Cu-Fe powder particles after mechanically alloyed for selected times of milling. The particle morphology was characterized using digital scanning electron microscope in the secondary electron image mode. After 1 h of milling, the powder particles of Cu and Fe were found to be nearly spherical shaped with an average size in the range of 20-100 μm “Figure 1a”. After 20 h of milling, the morphology became more homogeneous; due the mixing both the elemental powders in this step “Figure 1b”. An increase in the particle size is noticed, indicating the welding of the little particle to the surface of larger ones during subsequent milling. Further milling to 40 h leads to an increase in particle sizes “Figure 1c”. Figures 1d and 1e show the micrographs corresponding to big particles of alloy obtained after 60 and 80 h of milling where the cold-welding process clearly favours the agglomeration and the smooth appearance. The large agglomerated clusters consisting of smaller particles are apparent in the micrograph with a higher magnification. Figures 1f and 1g indicate that milling for 100 and 200 h were followed by significant particle refinement which led to formation of ~100 μm diameter particles. Higher magnification reveals that these 100 μm particles are agglomerates of smaller particles of around 30 μm. At this stage, fracturing has been the dominant process and particles seem to have uniform irregular shape. This brittle fracturing may be due to strain hardening induced by repeated welding, fracturing and re-welding of different constituent powder during milling process. EDX microanalysis of localized zones obtained after 100h of milling shows the oxygen contamination during sampling (Fig. 1h). This contamination can be on the surface of the powders and its quantity is small enough to be detected by XRD.

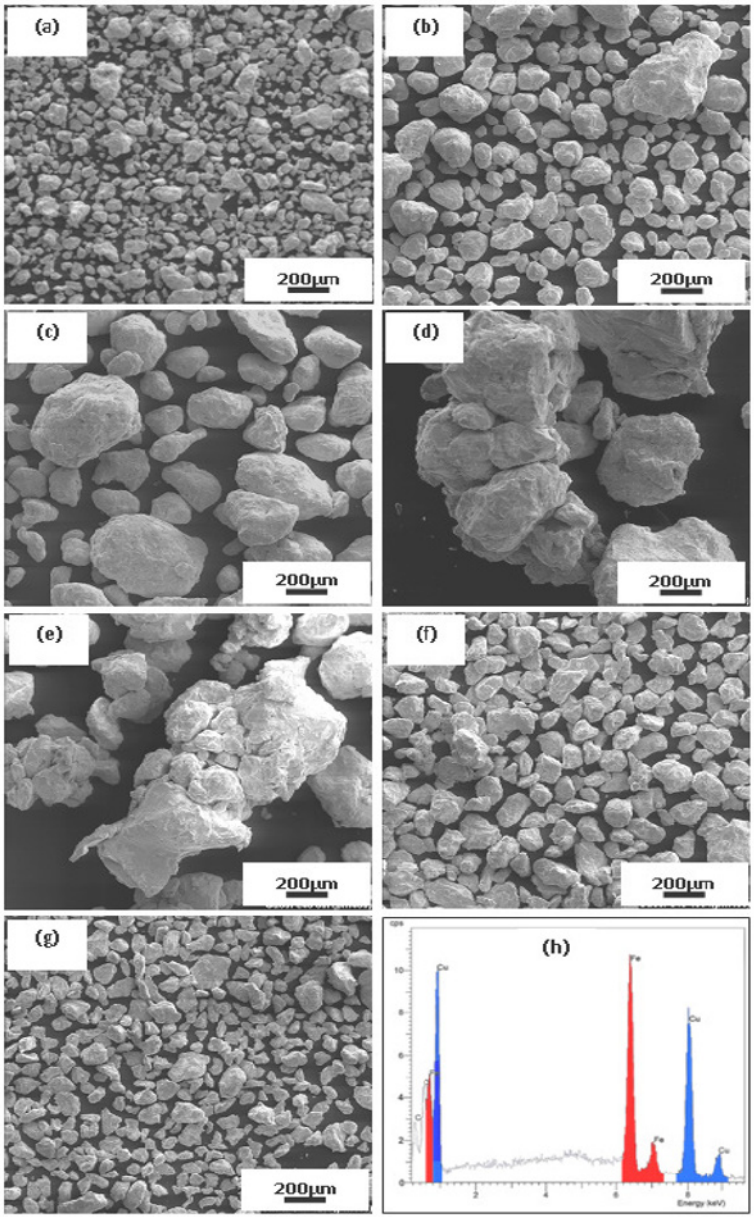

Fig. 1. Typical scanning electron micrographs (secondary electron image mode) corresponding to mechanically milled Cu-Fe powders (initial composition 60% Cu): (a) 1h, (b) 20h, (c) 40h, (d) 60h, (e) 80h, (f) 100h, (g) 120h and (h). The EDX corresponds to 100h.

3.2 X-ray diffraction pattern characteristics

Figure 2 depicts the X-ray diffraction patterns obtained for Cu-40%Fe powders as a function of milling time. The most noticeable features are the transformations occurring in the powder samples during milling. After MA for 1h, the recorded peaks correspond to the free FCC Cu (a_{Cu} = 3.6138 ±

0.0001 Å) and BCC Fe (a_{Fe} = 2.8656 ± 0.0001 Å). After 10 hours of milling, one can notice that the peaks specific to BCC iron phase become less intense and the Cu diffraction peaks profiles become asymmetric, broaden and displaced, demonstrating that Fe have gradually reacted with Cu to form supersaturated Cu(Fe) solid solution. The new contribution in the peak profiles can be due to appearance of this new phase which possesses the same structure as the FCC Cu, but is characterized by slightly larger unit cell parameter. The corresponding lattice parameters are a_{Cu}=(3.6434±0.0001)Å and $a_{Cu(Fe)}$ = (3.6466 ± 0.0001)Å.

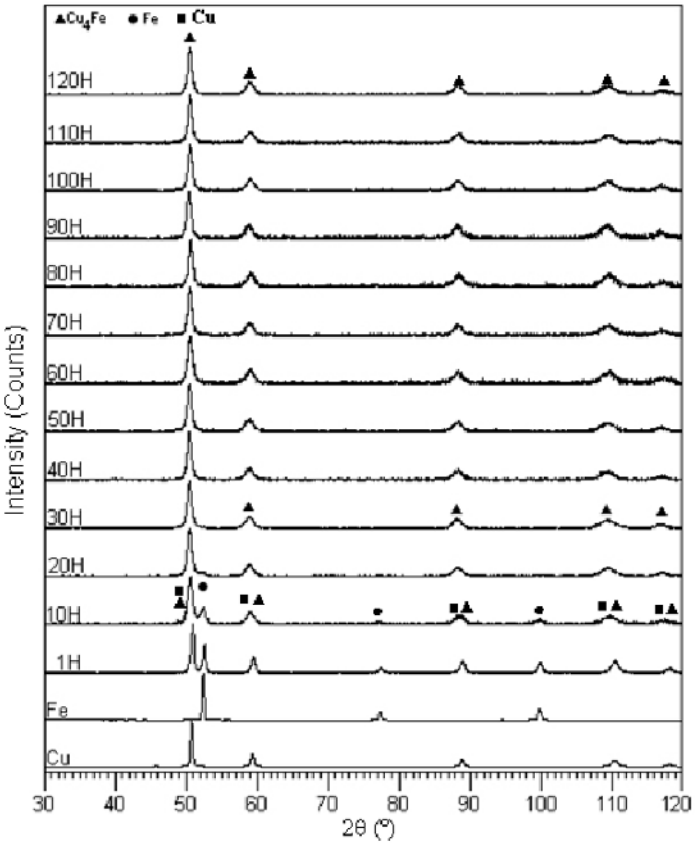

Fig. 2. XRD patterns of X-ray diffraction pattern of the MA Cu-Fe powders as a function of milling times.

After 20h of milling, a very small amount of iron is detected and this is deduced from the relatively low intensity of the peak $(110)_{Fe}$ and with a value of a_{Fe}=(2.8720± 0.0001)Å. After milling time for 30h, this peak disappears completely, whereas the remaining peaks become more symmetric and can be related to one Cu(Fe) FCC phase with a value of $a_{Cu(Fe)}$=(3.6482± 0.0001)Å. Prolonging the milling time to 120 h, these FCC peaks become more symmetrical and their positions remain almost unchanged. These facts can probably inform on the disorder-order transition that occurs when the FCC Cu(Fe) supersaturated solid solution transforms to intermetallic Cu-Fe phase (identified by Rietveld method to the FCC Cu_4Fe phase (space group: Fm-3m; a=(3.6515±0.0001)Å)). It is worth noting that the maximum of lattice parameters is for 40h of milling. The variation of the lattice parameter as a function of milling time can be correlated to the change in composition and/or to the lattice expansion due to the increase in the density of dislocations with their characteristic strain fields on the nanograin boundary [12,17,18]. The decrease of the amplitude and the increase of the broadening of the Bragg peaks with milling time can be explained by the contribution of the

effective crystallite size and an increase of the lattice strains. Figure 3 shows the dependence of the calculated crystallite size and lattice strains on the milling time. One can observe the sharp decrease of the crystallite sizes of Cu and Fe less than 120 nm after 1h of milling. It is worth noting that the character of nanocrystalline structure under certain conditions of deformation is dependent on the crystalline structure. For nanocrystalline structures observed in metals, the low crystallite size is explained by the competition between the levels of stress produced by a milling device, and the large degree of dynamic recovery in the milled material [19]. After that, the measured crystallite sizes diminish rapidly until reaching a value of about 10 nm after 20 and 30 h, for Fe and Cu, respectively. The lattice strains increase for both elements during the first hour of milling, followed by a slight increase. The Cu(Fe) supersaturated solid solution may well be the product of the solid state reactions with a crystallite size of 60 nm after 10h of milling. This might be related to the fact that during MA, the nanometer scaled diffusion couples are produced by high energy mechanical milling which involves plastic deformation, fracture and cold welding of powder particles. Thus the atomic diffusivity is enhanced through the creation of a large amount of structural defects. After 30 hours of milling, one can see a rapid decrease of the initial value of the mean crystallite to 15 nm, then a slight increase to reach a value of 19 nm after 50h of milling. This is most probably due to dynamic recrystallization of grains created by local heating during the mechanical alloying process [20]. After that, the Cu(Fe) crystallites are slightly refined as the milling time increases and reached a final value of about 13nm at 120 h of milling. On the other hand, the lattice strains the FCC Cu(Fe) phase, from its formation after 10 hours of milling with a value of $(\varepsilon^2)^{1/2}$=0.83 %, increases continually with increasing milling time until reaching a value $(\varepsilon^2)^{1/2}$=1.3 % after 90 h, then remains unchanged when increasing milling time to 120 h.

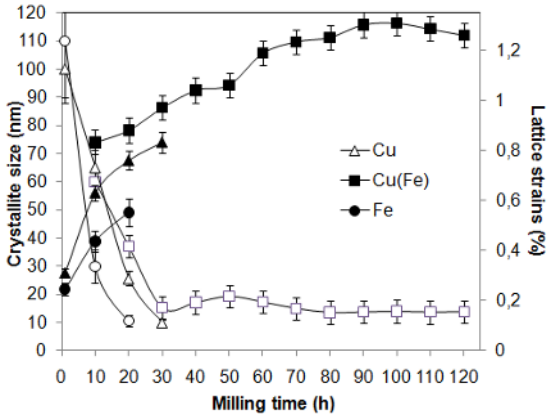

Fig. 3. Dependence of the microstructure parameters of the metallic phases on the milling time: the calculated crystallites sizes (Empty markers) and the calculated lattice strains (Full markers).

In general, lattice strains caused by MA are commonly attributed to the generation and movement of dislocations [21,22]. Moreover, Fecht [23] claimed that the generation and the movement of dislocations could decrease grain size. On the other hand, it is well known that the milling can lead other modifications: atomic site interchange [24] and vacancies [25]. The atomic site interchange can occur here due to the milling of two metal powders. During the whole MA process of powders, the lattice expansion is 1.04 %, therefore the formation of vacancies contradictorily be used as a proof to explain the present results. Hence dislocations are considered to be responsible for the final MA state. So, for MA samples, the density of dislocations, ρ, is represented in terms of the crystallite size, D and the lattice strains ε by [17]:

$$\rho_D = 2\sqrt{3}\frac{\langle \varepsilon^2 \rangle^{1/2}}{D.b} \quad (1)$$

where b is the burgers vector of dislocations, and equals 0.707×a for the FCC structure. The calculated dislocation density of the MA Cu(Fe) samples are represented in Fig.4. It is clearly seen that the mean dislocation density ρD increases rapidly from about 2.2×10^{16} m^{-2} to 6.7×10^{16} m^{-2} with increasing milling time from 10 to 30 h, then it shows a low diminution after 40 h of milling to a value of 6.05×10^{16} m^{-2}. This is most probably due to partial dynamic recrystallization. Usually, in conventional polycrystalline materials, the GBs are thought to be barriers to the dislocations motion; therefore, the slight decrease in the dislocations density within further milling time indicates a softening of the GBs. When the GBs have turned soft or relaxed, the amount of the dislocations piled up near the GBs will be decreased. At further milling time, one can see a slow increase of ρ_D to 7.4×10^{16} m^{-2} after 90h, and remain unchanged at a steady-state value. This can be related to accumulate strain hardening of the powder material during longer milling times.

The phase proportions as a function of milling time are also represented in Fig 4. One can see that the phase proportions of Cu and Fe decreases with increasing milling time, due to their continuous reactions. The phase proportion of the FCC Cu(Fe) phase, from its formation with a 19%, increases gradually with increasing milling time until reaching a value of 98% after 50 h, then remains unchanged when increasing milling time to 80h. This confirms the formation of the stable intermetallic compound Cu4Fe. After that, the proportion of Cu-Fe decreases slightly with increasing milling time to a value of 96%; this can be attributed to the order-disorder transition that occurs in the FCC Cu-Fe intermetallic when it is subjected to heavy deformation.

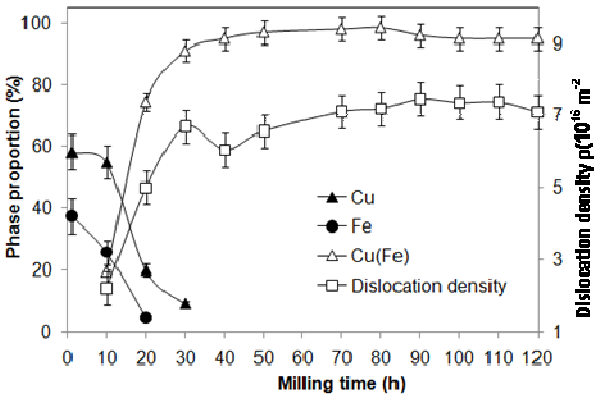

Fig. 4. Evolution of the phase proportions of the identified phases and the dislocations density as a function of milling time.

4 Conclusions

Nanocrystalline Cu(Fe) solid solution powder with crystallite of 13 nm has been successfully synthesized from the mixture of elemental Cu and Fe powders by high energy mechanical alloying process. At the early stage of the MA process, Cu(Fe) solid solution is formed firstly by the solution of Fe atoms into FCC Cu lattice. The single phase of FCC Cu(Fe) was formed after milling time exceeds 30 hours and the resulting powder has a nanometer scale structure. The character and the density of dislocations in FCC Cu(Fe) were determined. The dislocation densities were found to be 7.4×10^{16} m^{-2} and the strain broadening caused by high energy mechanical alloying is consistent with the concept of dislocations.

Acknowledgments

This work has been supported by Tunisian Ministry of Higher Education and Scientific Research and Joint Research Project Tunisia / Spain (AP/039058/11).

References

1. A.R. Yavari, P.J. Desre, T. Banameur, Phys. Rev. Lett., 68, **2235** (1992).
2. J. Eckert, L. Schultz, K. Urban. Appl Phys Lett. 55, **117** (1989).
3. C. Suryanarayana, Prog. in Mater. Sci. 46, **1** (2001).
4. D. Bahadur, R.A. Dunlap, M. Foldeaki, J Alloys Compd. 240, **278** (1996).
5. P.H. Shingu, K.N. Ishihara, K. Uenishi, J. Kuyama, B. Huang, S. Nasu, In: A.H. Clauer and J.J. de Barbadillo, Editors, Solid State Powder Processing, TMS, Warrendale, PA. **21** (1990).
6. K. Uenishi, K.F. Kobayashi, S. Nasu, H. Hatano, K.N. Ishibara, P.H. Shingu, Z. Metallk 83, **132** (1992).
7. J. Eckert, J.C. Holzer, W.L. Johnson, J Appl. Phys. 73, **131** (1993).
8. B. Majumdar, M. Manivel Raja, K.A. Narayanasamy, J Alloys Compd. 248, **192** (1997).
9. E. Gaffet, M. Harmelin, F. Faudot, J Alloys Compd. 194 (1), **23** (1993).
10. C. Domain, C. Becquart, Phys. Rev. B. 65 (2), **1**(2001).
11. C.S. Becquart, C. Domain, Nucl. Instrum. Methods Phys. Res. B. 202 (4) **44** (2003).
12. M. Mhadhbi, M. Khitouni, L. Escoda, J.J. Suñol, J Mater. Lett. 64, **1802** (2010).
13. T. Ungár, A. Borbèly, Appl. Phys. Lett. 69, **3173** (1996).
14. T. Ungár, I. Dragomir, Á. Rèvèsz, A. Borbèly, J Appl. Crystallogr., 32, **992** (1999).
15. S. Surinach, S. Gialanella, X. Amils, L. Lutterotti, M. D. Baro, ISMANAM-95. Schulz R, editor. Mater Sci Forum, 225, **395** (1996).
16. S. Gialanella, X. Amils, M.D. Baro, P. Delcroix, G. LeCaër, L. Lutterotti, S. Surinach, Acta Mater. 46, **3305** (1998).
17. M. Mhadhbi, M. Khitouni, L. Escoda, J.J. Sunol, M. Dammak, J. Nanomaterials, doi:10.1155, **712407** (2010).
18. L. Dekhil, S. Alleg, J.J. Sunol, J.M. Grenèche, Adv. Powder Techn. 20, **593** (2009).
19. A.I. Salimon, A.M. Korsunsky, A. N. Ivanov, J Mater. Sci. Eng. A 271, **196** (1999).
20. Q. Zeng, I. Baker, Intermetallics 14, **396** (2006).
21. F. A. Mohamed, Acta Mater. 51, **4107** (2003).
22. M.P.C. Kalita, A. Perumal, A. Srinivasan, J Magn. and Magn. Mater. 2780-2783 **320** (2008).
23. H.J. Fecht, Nanostruct. Mater.6 (1–4), **33** (1995).
24. G. Liang, J. Huot, R. Schulz, J Alloys Compd. 320 (1), **133** (2001).
25. T. Helander, J. Agren, Acta Mater. 47, **1141** (1999).